

Highly Sensitive Sensors for the Detection of Nitro Compounds Based on Pyrene Labeled Dendrons

Andrea Ruiu¹ · Mireille Vonlanthen¹ · Pasquale Porcu¹ · Israel Gonzalez-Méndez¹ · Ernesto Rivera¹

Received: 12 July 2017 / Accepted: 20 September 2017 / Published online: 30 September 2017
© Springer Science+Business Media, LLC 2017

Abstract In this paper, we describe the synthesis and characterization of four novel pyrene labeled compounds, some of them dendritic, which can act as potential sensors for the detection of nitro compounds in methanol solution. Methanol was selected as solvent due to its polar properties, which provide similar characteristics to water. The obtained pyrene labeled molecules (PyOH, Pytb, PyNK1OH and PyNK1tb) were studied by UV–Vis and steady state fluorescence spectroscopy. Their application as sensors has been tested with three different nitro compounds: nitrobenzene, 1-chloro-2,4-dinitrobenzene and nitromethane. PyOH and Pytb showed a detection concentration limit for the analyzed quenchers in the order of nM, making these compounds suitable for high-sensitive sensing. PyNK1OH and PyNK1tb displayed high sensibility at μM concentration. All the sensors showed an accurate response towards quencher analytes.

Keywords Pyrene · Dendrons · Sensor · Quenching · Nitro compounds

1 Introduction

The development of sensors for nitro compounds has attracted the attention of many scientists and has been

improved in the last years [1–4]. Nitro compounds, in particular nitroaromatic molecules, represent a main risk for biological organisms [5]. Nowadays, the most common methods for their detection are X-ray imaging [6], ion mobility spectroscopy [7], gas chromatography mass spectroscopy (GC–MS) [8, 9], surface enhanced Raman spectroscopy [10, 11], and electrochemical methods [12, 13]. Although the good sensibility of these techniques, the development of new fluorescent methods for nitro compounds is ongoing, thanks to their portability and ease of use. For instance, metal organic frameworks (MOFs) [14, 15], nanomaterials [16], conjugated polymers [17–20], fluorescent dyes [4, 21] have showed good performance as fluorescent sensors for the detection of nitroaromatic pollutants, exhibiting a good sensibility on the detection of these contaminants.

Pyrene is one of the most studied fluorescent probes due to its outstanding photophysical properties such as high quantum yield, well defined absorption and emission bands, long lifetime and the ability to form excimers. This is just a brief list of the properties which allow an extensive study of pyrene-labeled molecules [22, 23]. Indeed, pyrene has been incorporated in a large variety of chemical structures, such as peptides [24, 25], oligothiophenes [26–28], molecules exhibiting energy transfer [29–32] and in MOFs [33, 34]. In addition, pyrene has been used as sensor for different pollutants, due to its high sensibility to the presence of quenchers [35–37]. In particular, it has been employed as probe for nitro compounds [38], oxygen [39, 40], heavy atoms [41, 42] and amines [43, 44].

Usually the quenching by nitro compounds on fluorescence emission is due to a PET mechanism (photo-induced electron transfer) [3]. This mechanism occurs because of the donor–acceptor interaction between electron rich fluorophore (pyrene) and electron poor group (nitro compound). In this phenomenon, the electron in the excited state of the

Electronic supplementary material The online version of this article (doi:10.1007/s10904-017-0686-6) contains supplementary material, which is available to authorized users.

✉ Ernesto Rivera
riverage@unam.mx

¹ Instituto de Investigaciones en Materiales, Universidad Nacional Autónoma de México, Circuito Exterior Ciudad Universitaria, C.P. 04510 Ciudad de México, Mexico

fluorophore is transferred to the ground state of the nitro compound so that this electron transfer leads to the formation of an excited complex. This specie usually returns to ground state without a photon emission, except in some cases, where an exciplex emission is detected.

An interesting way to modulate the sensitivity of luminescent-labeled sensors is to modify their peripheral structure. In this work, we decided to modify the outer structure by functionalizing the pyrene substrate with the Behera's amine [45–48] in order to obtain a dendritic system similar to those developed by Newkome. This specific dendritic structure has been studied by labeling using different derivatives as photosensitizers [49–52] and it has been used in biological devices [53–56], as drug delivery agent [57–59] and for surface modification [60–62]. Thanks to this particular amine, the synthesis of dendritic systems became much easier, with a simple method of coupling-cleavage. The peripheral groups can be trivially functionalized, allowing us to obtain a water soluble or a more apolar system.

In this work, we report the synthesis of four novel pyrene-labeled molecules and the study of their quenching behavior in the presence of three different nitro compounds [nitrobenzene (**NB**), dinitrochlorobenzene and nitromethane (**NM**)] in methanol. These pyrene-labeled compounds showed to be suitable sensors for this kind of pollutants.

2 Experimental

2.1 Materials

Pyrenbutyric acid (PyOH, 97%, Sigma Aldrich), tert-butylamine (98%, Sigma Aldrich), *N,N'*-dicyclohexylcarbodiimide (DCC, 99%, Sigma Aldrich), 4-(dimethylamino)pyridine (DMAP, 99%, Sigma Aldrich), formic acid (95%, Sigma Aldrich), aminotriester (Frontier Scientific), **NB**, (99%, Sigma Aldrich), 1-chloro-2,4-dinitrobenzene (**DNB**, %97, Sigma Aldrich), **NM** (99%, Sigma Aldrich) were employed as starting materials. Methanol (HPLC grade) was used in the spectroscopical studies.

2.2 Synthesis of the Pyrene Derivatives

2.2.1 *N*-(*tert*-butyl)-4-(pyren-1-yl)butanamide (Pytb)

Pyrenebutyric acid (0.1 g, 0.34 mmol) was dissolved in 20 mL of CH₂Cl₂ with DCC (0.078 g, 0.38 mmol), DMAP (0.005 g, 0.04 mmol) and tertbutyl amine (0.028 g, 0.38 mmol). The solution was stirred at room temperature under nitrogen atmosphere. After 48 h, the solution was filtered and purified by column chromatography (SiO₂, hexane:ethyl acetate 2:1). The final product was obtained as a white powder (0.098 g, 83%). ¹H NMR (CDCl₃):

δ 1.34 (s, CCH₃, 9 H), δ 2.20 (m, CH₂CH₂CO, 4 H), δ 3.41 (t, PyCH₂, 2 H), δ 5.19 (s, CONH, 1 H), δ 7.87–8.33 (m, Py, 9 H). ¹³C NMR (CDCl₃): δ 27.00 (CH₂), δ 28.35 (CH₃), δ 32.15, 36.40 (CH₂–CH₂), δ 36.68 (CH₂), δ 50.67 [C(CH₃)₃], δ 122.96, δ 124.28, δ 124.41, δ 124.60, δ 125.36, δ 126.20, δ 126.87, δ 126.93, δ 126.99, δ 128.31, δ 129.42, δ 130.42, δ 130.93, δ 135.54 (pyrene), δ 171.34 (CONH) ppm.

2.2.2 *Di-tert-butyl*4-(3-(*tert*-butoxy)-3-oxopropyl)-4-(4-(pyren-1-yl)butanamido) heptanedioate (PyNK1tb)

Pyrenebutyric acid (0.2 g, 0.68 mmol) was dissolved in 20 mL of CH₂Cl₂ with DCC (0.156 g, 0.76 mmol), DMAP (0.01 g, 0.08 mmol) and aminotriester (0.315 g, 0.76 mmol). The reaction mixture was stirred at room temperature under nitrogen atmosphere for 1 week. The solution was filtered and purified by column chromatography (SiO₂, hexane:ethyl acetate 2:1). The final product was obtained as a white powder (0.377 g, 81%). ¹H NMR (CDCl₃): δ 1.40 (s, CCH₃, 27 H) δ 2.00 (t, CCH₂, 6 H), δ 2.20 (m, PyCCH₂CCO–CH₂COOt_b, 10 H), δ 3.40 (t, PyCH₂, 2 H), δ 5.91 (s, CONH, 1 H), δ 7.83–8.33 (m, Py, 9 H). ¹³C NMR (CDCl₃): δ 27.38 (CH₂), δ 27.90 (CH₃), δ 29.79, δ 29.88 (CH₂–CH₂), δ 32.68 (CH₂), δ 36.68 (CH₂), δ 57.27 [C(CH₂–CH₂)₃], δ 80.51 [C(CH₃)₃], δ 123.24, δ 124.59, δ 124.62, δ 124.69, δ 124.83, δ 124.93, δ 125.65, δ 126.48, δ 127.24, δ 127.32, δ 128.59, δ 129.57, δ 130.76, δ 131.24, δ 135.77 (pyrene), δ 171.96 (CONH), δ 172.77 [COOC(CH₃)₃] ppm.

2.2.3 4-(2-Carboxyethyl)-4-(4-(pyren-1-yl)butanamido) heptanedioic acid (PyNK1OH)

PyNK1OH (0.2 g, 0.29 mmol) was dissolved in CH₂Cl₂ (5 mL) and formic acid (10 mL). The reaction mixture was stirred at room temperature under nitrogen atmosphere. After 48 h, it was concentrated at reduced pressure and the obtained red oil was washed until it became a yellow solid. This compound was dissolved in boiling acetone and then cooled down. The pure product was obtained as a white powder (0.150 g, 99%). ¹H NMR (CD₃OD): δ 2.07 (t, CCH₂, 6 H), δ 2.20 (q, PyCCH₂CCO, 2 H), δ 2.32 (t, CH₂COOt_b, 6 H), δ 2.38 (t, PyCH₂, 2 H), δ 5.19 (s, CONH, 1 H), δ 7.92–8.37 (m, Py, 9 H). ¹³C NMR (CD₃OD): δ 27.38 (CH₂), δ 29.79, δ 29.88 (CH₂–CH₂), δ 32.68 (CH₂), δ 36.68 (CH₂), δ 57.27 [C(CH₂–CH₂)₃], δ 80.51 [C(CH₃)₃], δ 123.24, δ 124.59, δ 124.62, δ 124.69, δ 124.83, δ 124.93, δ 125.65, δ 126.48, δ 127.24, δ 127.32, δ 128.59, δ 129.57, δ 130.76, δ 131.24, δ 135.77 (pyrene), δ 174.96 (CONH), δ 176.77 [COOH] ppm.

2.2.4 Materials

^1H and ^{13}C NMR spectra of these compounds in CDCl_3 and CD_3OD solution were recorded at room temperature on a Bruker Avance 400 MHz spectrometer, operating at 400 and 100 MHz for ^1H and ^{13}C , respectively. For UV–Vis and fluorescence experiments, methanol spectrum grade was purchased from Aldrich. The absorption spectra of the final compounds in solution were recorded on a Unicam UV300 UV/Vis spectrophotometer using 1 cm quartz cells and solute concentrations of $1\text{--}3 \times 10^{-5}$ M for the dendritic compounds. It has been verified that the Beer–Lambert law applies for the used concentrations. Fluorescence spectra corrected for the emission detection were recorded on a Fluorolog 3 Horiba spectrofluorometer with a Xenon lamp as light source. The slits widths were set to 1 nm on excitation and 1 nm on emission. Each solution was excited at 342 nm, using a 1 cm quartz cell. For all compounds, a pyrene concentration of 2.5×10^{-6} M was employed to ensure that the solutions would have an absorbance of 0.1 at 342 nm in order to avoid any inner filter effect; the samples were excited at 342 nm. The fluorescence cells were cleaned with a solution of ammonium persulphate in concentrated sulphuric acid before use. Fresh solvent was used each day and checked for pyrene contamination prior to the preparation of the samples. Before recording the emission spectra, methanol solutions of the compounds were first degassed for 5 min and recorded on the spectrophotometer.

2.2.5 Samples Preparation

To prepare the analyzed solutions, different starting solutions were prepared with methanol (HPLC grade). These stock solutions were prepared to give a concentration of 1.25×10^{-1} M (PyOH=0.360 g in 10 mL; Pytb=0.429 g in 10 mL; PyNK1OH=0.714 g in 10 mL; PyNK1tb=0.857 g in 10 mL). Then, the solutions were diluted up to a concentration of 1.25×10^{-4} M. Then, from each solution, 10 μL were brought to a volume of 5 mL in order to obtain a final concentration of 2.5×10^{-6} M.

The nitro compounds stock solutions were prepared similarly. Initially, we prepared solutions with a concentration of 5×10^{-1} M (NB=0.615 g in 10 mL; NM=0.305 g in 10 mL; DNB=1.012 g in 10 mL). Then, these solutions were diluted respectively up to 5×10^{-4} M and then diluted until a concentration of 5×10^{-6} M was obtained.

To prepare nM analyzed solutions, 10 μL of pyrene-labeled compound solution and 10 μL of nitro compound stock solution (5×10^{-6} M) were added into a volumetric flask and brought to a volume of 5 mL to obtain a 10 nM concentration solution. Then, similar solutions were prepared by adding from 10 to 1000 μL of nitro compound stock solution in order to increase the nitro concentration.

To prepare μM analyzed solutions, 10 μL of pyrene-labeled compound solution and 10 μL of nitro compound stock solution (5×10^{-4} M) were added in a volumetric flask and brought to a volume of 5 mL to give a 1 μM concentration solution. After that, similar solutions were prepared by adding from 10 to 800 μL of the nitro stock solution in order to increase the nitro concentration.

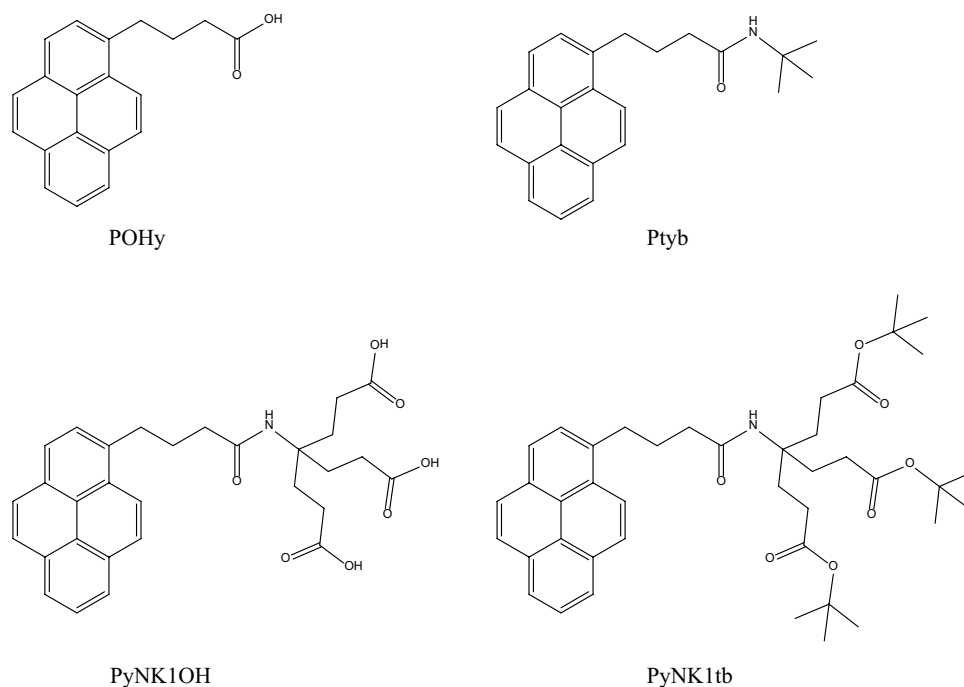
3 Results and Discussion

3.1 UV–Vis and Steady State Fluorescence Studies in the Absence of Quencher

The obtained compounds proposed as sensors in this work are shown in Fig. 1. Their synthesis and structural characterization is presented in the experimental part. The optical and photophysical properties of the designed molecules were studied by absorption and fluorescence spectroscopy. The maximum absorption wavelength (λ_{max}), molar extinction coefficient (ϵ), emission wavelength (λ_{em}) and fluorescence intensity (F.I.) of all compounds are summarized in Table 1.

The absorption spectra were obtained in methanol solution with a concentration of 2.5×10^{-5} M. All the samples exhibited ϵ values that goes from 4.2×10^4 to 4.8×10^4 , with a little increase between the zero generation and the first generation. The absorption spectra exhibit the typical $S_0 \rightarrow S_3$ and $S_0 \rightarrow S_2$ transitions of pyrene, at 275 and 342 nm, respectively, showing a hypsochromic shift with respect to less polar solvents; these wavelengths are typical for aqueous solutions of pyrene labeled systems [44]. The peak-to-valley ratio, equal to 3.3 for all the samples, clearly reveals the absence of pyrene–pyrene interactions, which prevents the formation of excimers.

The steady state spectra of the dendritic compounds were recorded in methanol solution, exciting at 342 nm at room temperature, with a concentration of 2.5 μM . The emission spectra of the compounds are shown in Fig. 2. All compounds exhibited maximum emission at 375 nm. The fluorescence intensity increases from the acid derivatives to the tertbutyl esters: in generation zero, the intensity augments from 2.36×10^6 to 2.59×10^6 , showing an increase of ca. 10%. However, in the first generation dendron, it augments from 2.21×10^6 to 2.73×10^6 , showing an emission rise of about 20%. This phenomenon suggests an interaction between pyrene and the terminal group (carboxylic acid and tertbutyl ester). A significant change in the pyrene environment was noticed by calculating I_1/I_3 ratio in the emission of the pyrene dendrons. In fact, this ratio was considerably lower for the tertbutyl ester derivatives, thereby confirming an effective influence of the terminal groups on pyrene fluorescence behavior. These considerations allow us to affirm the presence of an “umbrella effect”, which can be

Fig. 1 Structure of pyrene labeled molecules**Table 1** Optical properties of the pyrene derivatives: UV–Vis and fluorescence parameters

	ϵ (cm ⁻¹ M ⁻¹)	$\lambda_{\text{abs}}^{\text{max}}$ (nm)	$\lambda_{\text{em}}^{\text{max}}$ (nm)	F.I. ^a (a.u.)	I_1/I_3 ^b
PyOH	42 812	342	375	2.36×10^6	2.65
Pytb	44 547	342	375	2.59×10^6	2.44
PyNK1OH	48 723	342	375	2.21×10^6	2.52
PyNK1tb	45 407	342	375	2.73×10^6	2.31

^aFluorescence intensity^b I_3 at 386 nm

relevant to evaluate the performance of these molecules as quencher sensors, in particular because of the sensitivity of these compounds.

3.2 Fluorescence Quenching

In order to study the behavior of the pyrene derivatives in the presence of nitro groups, we decided to use three different nitro compounds usually employed in an organic synthesis laboratory as analytes: **NB**, 1-chloro-2,4-dinitrobenzene and **NM**. These compounds are very toxic, due to their carcinogenic effects and they cause irritation if they enter into contact with skin and respiratory ways [63, 64].

The dendron generation response was studied using different quencher concentrations. Zero generation response (PyOH and Pytb) was analyzed in the presence of a very low concentration of quencher, specifically from 10 nM to 1 μ M. Unlikely, first generation (PyNK1OH and PyNK1tb)

response was studied at higher concentrations of quencher, from 1 to 80 μ M. The influence of the quencher on the fluorescence will be discussed separately for each dendron. In order to verify the differences between all dendritic compounds, we have taken into account two different parameters: namely, when I_q/I_0 is equal to 0.5 and when the quenched emission reaches a stationary value and does not change any more even by adding larger amounts of quencher.

3.2.1 PyOH in the Presence of Quencher

We started our study using a commercially available compound, pyrenbutyric acid (PyOH) as sensor and **NB** as detection target or quencher. The presence of **NB** causes a quite fast decrease in fluorescence intensity, where the emission diminishes to a half just using a 75 nM solution of quencher. On the other hand, the fluorescence intensity reaches a stationary state at a concentration of 300 nM, showing a significant quenching. The emission at this point decreased about 30% with respect to that observed in the absence of quencher.

The second analyzed nitro compound was 1-chloro-2,4-dinitrobenzene (**DNB**) (Fig. 3), which exhibited a significant quenching about 50%, more rapidly than **NB**, at a concentration of 50 nM. The quenching equilibrium is attained faster than in the case of **NB**, with a concentration of 100 nM. This remarkable difference can be attributed to the presence of two nitro groups in the aromatic ring, which provokes a more effective quenching of the pyrene emission.

The third quencher tested in this study was **NM**. This compound was supposed to exhibit the highest quenching

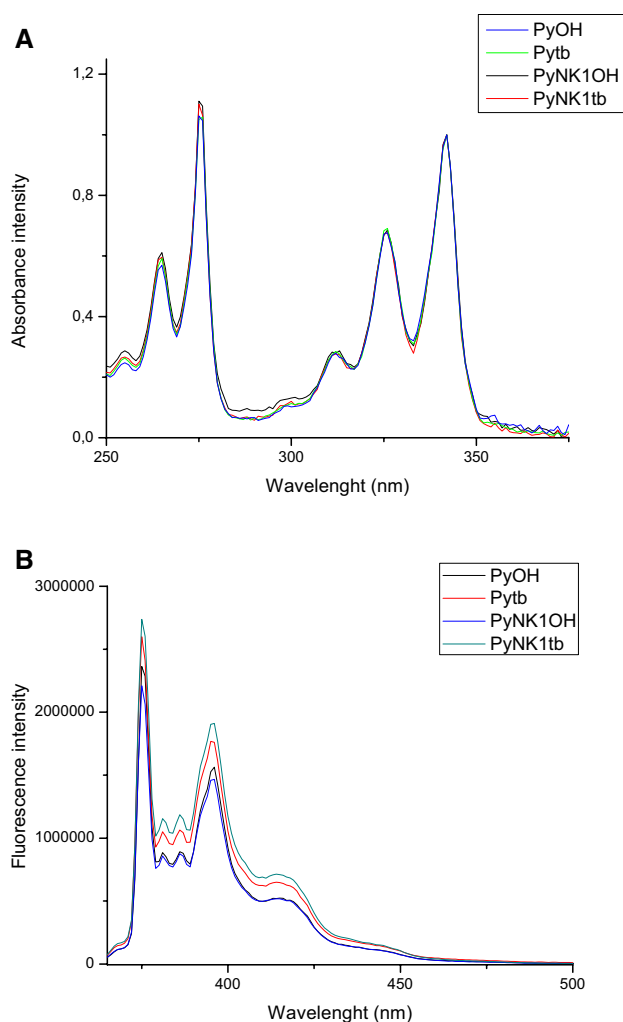


Fig. 2 UV-Vis (a) and steady state fluorescence spectra (b) of: PyOH, Pytb, PyNK1OH, PyNK1tb

efficiency due to its small size. This hypothesis was confirmed by the fluorescence analysis: 50% quenching of the fluorescence intensity was achieved at lower concentration than with the other quencher, to be precise at a concentration of 20 nM of **NM**. Instead, a plateau was reached at a quencher concentration of 100 nM, like in the case of **DNB**.

3.2.2 Pytb in the Presence of Quencher

The second proposed sensor was Pytb, which was used like PyOH for the detection of the nitro compounds by quenching.

NB shows a good quenching power on this dendron since the fluorescence decreases 50% at a nitro compound concentration of 200 nM in methanol. In this case, the 50% value represents the highest intensity of quenching reached for this kind of sensor. The presence of a tertbutyl group in periphery caused that the total achieved quenching was

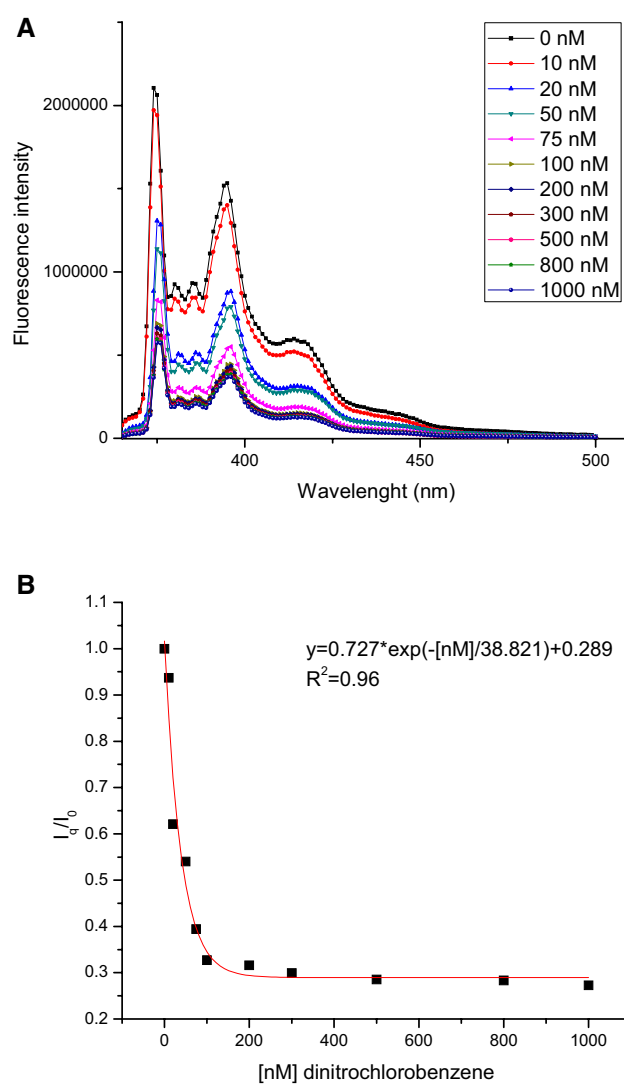


Fig. 3 Steady state (a) and I_q/I_0 ratio (b) in function of amount of **DNB** for PyOH

50% of emission, instead of 30% like with the acid derivative. This can be attributed to the increased steric hindrance of the dendritic structure because of the tertbutyl group, which make more difficult the encounter between the pyrene chromophore and **NB**.

In this case, despite the presence of two nitro groups **DNB** quenching seems to be as efficient as that of **NB**. As we have previously observed, the total quenching resulted to be 50% and it was achieved at a concentration of 200 nM. Moreover, the I_q/I_0 ratio showed some irregularities, in particular with low concentrations of the analyte. This consideration allows us to affirm that this molecule is not a good sensor for this quenching system.

At last, the **NM** sensing exhibits an interesting behavior, since the quenching seems to reach a first equilibrium at a concentration of 100 nM, leading to a quenching about

40% of the initial emission. Then, the emission continues decreasing by adding more quencher agent up to concentration of 1 μM , which was fixed as superior limit for this generation. As we explained before, this faster quenching is due to the smaller size of **NM**. Further emission reduction can be explained by gradual conformational changes in the sensor structure in the presence of a higher amount of the small quencher **NM**.

3.2.3 Comparison Between PyOH and Pytb

All the previously discussed results are summarized in Table 2. Emission spectra and the I_q/I_0 vs quencher concentration graphs are included in the Supporting Information. The main structural difference between PyOH and Pytb is the presence of a tertbutyl as terminal group in the chain, which acts as pyrene protector. This effect results in an increase on the detection limit of quencher concentrations (Fig. 4). On the other hand, the total quenching was reduced by the presence of the tertbutyl moieties. In fact, the PyOH is quenched to 30% of initial intensity by all the quenchers; instead Pytb only to 50% of its initial emission intensity. An important observation for all these compounds used as nitro compound sensors, is the high detection sensitivity, which is in order of 10–15 nM. These values are close to that suggested by EPA as recognition limit for real applications.

3.2.4 PyNK1OH in the Presence of Quencher

We studied the ability of the first generation dendron as sensor; it was found a lack of response at nanomolar quencher concentrations. In fact, the range of studied concentrations goes from 1 to 80 μM . Like the previously studied sensors, the sensing efficiency of PyNK1OH and PyNK1tb was tested in the presence of **NB**, 1-chloro-2,4-dinitrobenzene (**DNB**) and **NM**.

PyNK1OH shows a fast response towards the presence of **NB** exhibiting a decrease in emission intensity equal to 5% at a concentration of 1 μM . The 50% quenching was achieved between 7 and 10 μM , displaying a good range of analysis. The quenching equilibrium was reached at 15 μM , with a fluorescence reduction of 30% with respect to the non-quenched one. Even by increasing generously the amount of **NB** up to 80 μM the quenching process

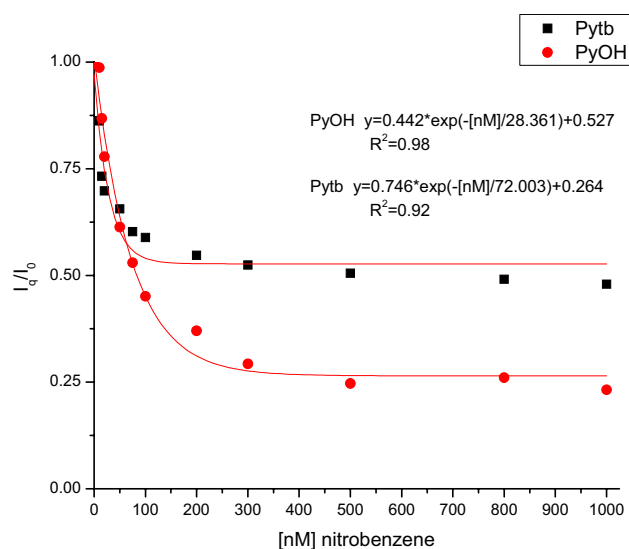


Fig. 4 I_q/I_0 ratio in function of **NB** amount for PyOH and Pytb

remains constant, showing that the reduction to 30% of the initial emission is the maximum decrease in fluorescence intensity for this dendron.

The **DNB** exhibited a similar effect like **NB** on PyN-K1OH fluorescence, where there is an intense quenching up to 1.5 μM , equal to an emission decrease of 20%. After this diminution, 50% quenching was surprisingly obtained at 15 μM , a higher concentration than that of **NB**. The maximum quenching value attained with this sensor was 55%, compared to the non-quenched dendron (Fig. 5). This can be due to electrostatic repulsions between the partially charged nitro groups and the carboxylic groups present the dendron branches, which are very close to the pyrene moiety, making more difficult for the quencher to encounter the fluorescent chromophore.

Due to its smaller size, **NM** causes a decrease in fluorescence intensity of 45% at 1.5 μM . Then, the 50% quenching was rapidly obtained at 3 μM , a lower concentration than that used with the other quencher. The quenching equilibrium was reached at 10 μM , with an emission equal to 31% of the starting one. As we mentioned before, the small size of **NM** allows overcoming the steric hindrance, thereby permitting a rapid quenching of the pyrene emission.

Table 2 Comparison between PyOH and Pytb in function of the quencher

Sample	NB		DNB		NM	
	50% quench. (nM)	Maximum detection	50% quench. (nM)	Maximum detection	50% quench. (nM)	Maximum detection
PyOH	75	300 nM	50	100 nM	20	100 nM
Pytb	200	–	200	–	100	–

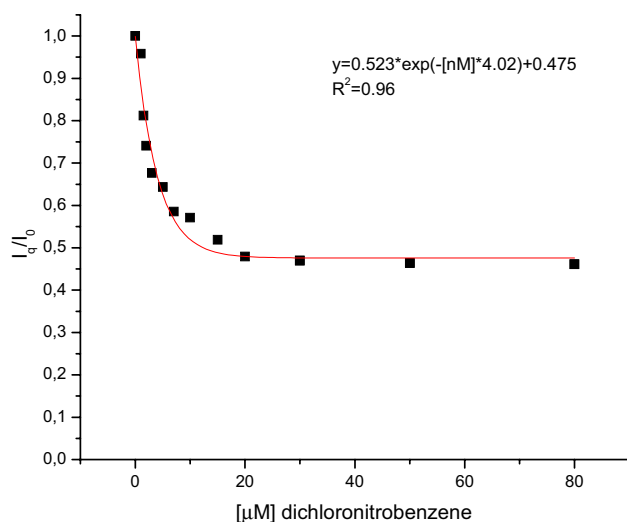


Fig. 5 I_q/I_0 ratio in function of the **DNB** amount for PyNK1OH

3.2.5 PyNK1tb in the Presence of Quencher

For the first generation dendrons, we proposed an alternative tertbutyl end-capped compound (PyNK1tb) to make a comparison with PyNK1OH. PyNK1tb exhibits a wide detection limit for **NB**. The first decrease at 1 μM is equal to 7%; after this concentration the decrease does not reach a real equilibrium. In fact, the quenching is proportional to the nitro compound concentration until a superior limit of 80 μM , as we can observe in Fig. 6. This gradual decrease allows an effective detection of **NB** along the analyzed range of concentrations.

The **DNB** quenching showed a fast-initial quenching of 11% in the non-quenched emission at 1 μM . The 50% decrease in fluorescence intensity of the PyNK1tb sensor was achieved at 15 μM . With a further increase of **DNB**, the emission declined slowly until 30% with respect to the initial emission at 80 μM . This different behavior in sensing **DNB**, compared to **NB**, is due to the strong quenching power of the dinitroaromatic system.

Similarly, **NM** causes a fast quenching of PyNK1tb fluorescence; to be precise at 1.5 μM the emission is reduced to 70% with respect to the initial emission in the absence of quencher. The 50% quenching was achieved at a quencher concentration of 10 μM . The equilibrium was reached at 30 μM , when the emission decreased to 36% compared to the pure sensor. This range of 30 μM is larger related to **DNB** and this increased detection limit is undoubtedly due to the smaller dimension of **NM**.

3.2.6 Comparison Between PyNK1OH and PyNK1tb

The emission spectra and the I_q/I_0 versus quencher amount graphs are included in the Supporting Information. Both

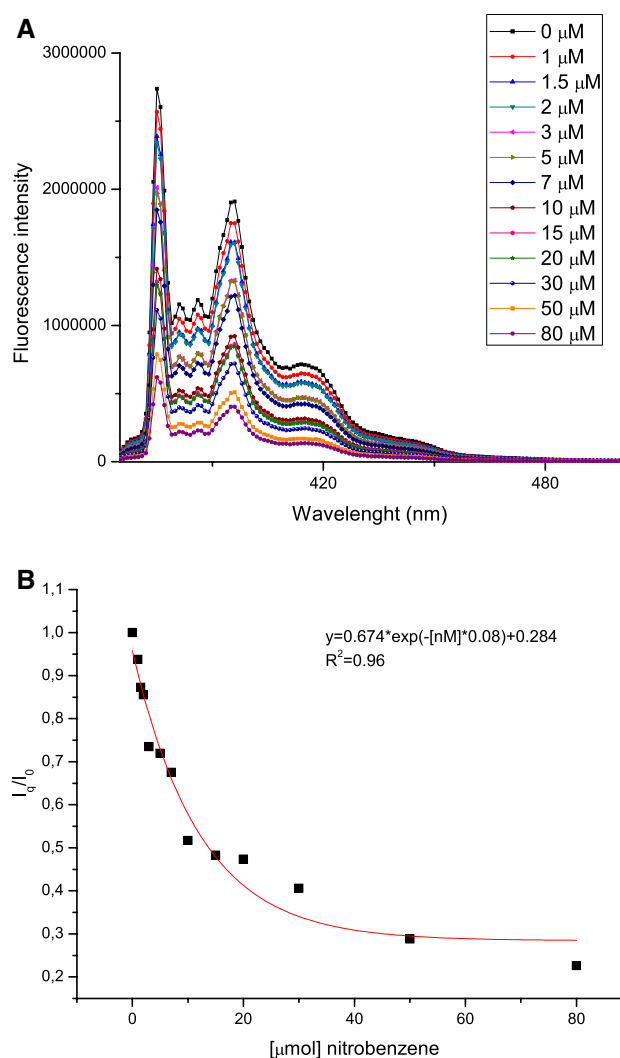


Fig. 6 Steady state (a) and I_q/I_0 ratio (b) in function of the **NB** amount for PyNK1tb

sensors showed similar response to the different analyzed quencher, as shown for **NB** quenching (Fig. 7). The inferior detection limits and the initial quenching are close for both sensors in each study, but usually the dendron bearing tertbutyl terminal groups exhibits higher regression constant values. The response towards the presence of nitro groups does not afford a clear equilibrium and the emission continues diminishing even at higher concentrations of quencher.

According to the classical mechanism there is a photo-induced electron transfer (PET) from the donor group (pyrene derivative) to the acceptor (nitro compound). In a typical PET The excited state of the donor fluorophore (pyrene derivative) donates an electron to the ground state of the acceptor (nitro compound) thereby forming a complex, which return to the ground state without the emission of a photon. Then, the additional electron on the acceptor returns to the donor group. The energy gap between the LUMO of

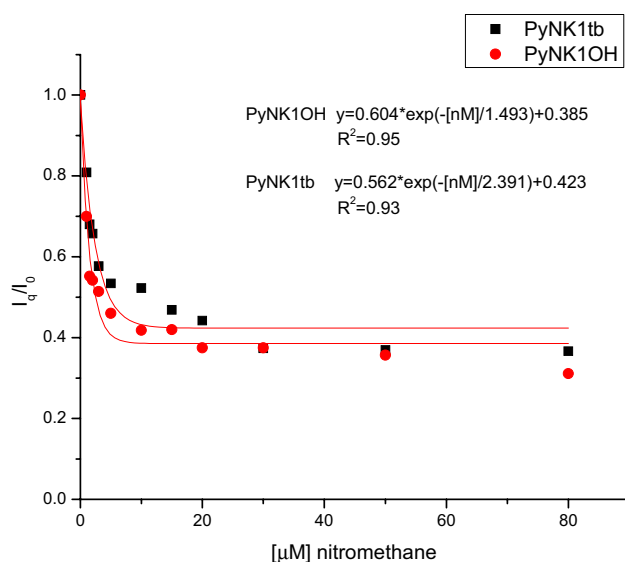


Fig. 7 I_q/I_0 ratio in function of amount of NM for PyNK1OH and PyNK1tb

the donor (pyrene derivative) and that of the acceptor (nitro compound) thermodynamically allows this process so that the quenching efficiency depends on a big measure on the electron transfer [3].

The fluorescence quenching requires the molecular interaction between the fluorophore (pyrene derivative) and the quencher (nitro compound) by diffusion giving rise to a dynamic complex, which is the case in our systems. Since the donor (pyrene derivative) and the acceptor (nitro compound) are located in different molecules and separated in the medium. When both donor and acceptor groups are located in the same molecule the formation of static complexes is possible. Dynamic and static complexes can be distinguished by life time decays, concentration, viscosity, temperature effects [3].

In our systems, it is evident that we have a dynamic quenching mechanism since the fluorophore (pyrene) and the quencher (nitro compound) are situated in different molecules; their interaction is totally by diffusion in solution and strongly depends on the concentration of the species. We can observe a variation of the fluorescence intensity of the donor (pyrene) in function of the added amount of acceptor (nitro compound) until we reach a stationary state. The detection sensibility varies in function of the structure of our sensors and the size and number of nitro groups present in the quenchers.

4 Conclusions

In this work we described the synthesis and characterization of four pyrene labeled compounds, some of them dendritic,

for the detection of nitro compounds in methanol solution, to be specific: **NB**, 1-chloro-2,4-dinitrobenzene and **NM**. The dendrons possess different size and terminal groups, having two different generations and the presence of acid or tertbutyl terminal groups in the periphery. The resulting compounds showed diverse responses depending on the size and the terminal groups: the generation zero sensors showed a decrease in fluorescence intensity at nM concentrations of quencher, giving a good linear correlation constant up to 1 μ M concentration. The first-generation sensors showed a higher detection limit; their response was significant in μ M concentration for all the nitro analytes. On the other hand, PyNK1OH and PyNK1tb exhibited good correlation constants. The good response to the quencher presence makes these pyrene labeled compounds potential sensors for nitro compounds. Thanks to the easy synthetic and purification methods and the good response towards different concentrations of quenchers, these pyrene labeled Newkome type dendrons may be used as potential candidates for the detection of explosives based on nitro compounds. As expected, the quenching process occurs via a dynamic mechanism.

Acknowledgements We thank Miguel A. Canseco Martínez and Gerardo Cedillo for their technical assistance in the characterization of the sensing compounds. We are also grateful to CONACYT (Project 253155) and PAPIIT (Project IN-100316) for financial support. Mireille Vonlanthen is grateful to the Swiss National Science Foundation for a postdoctoral fellowship (P2ZHP2-148707). A. Ruiu, P. Porcu and I. González-Méndez thank Posgrado en Ciencias Químicas UNAM and CONACYT for scholarship and financial support, respectively.

References

1. A. Azhdari Tehrani, L. Esrafil, S. Abedi, A. Morsali, L. Carlucci, D.M. Proserpio, J. Wang, P.C. Junk, T. Liu, *Inorg. Chem.* **56**, 1446 (2017)
2. Y. Sun, J. Liu, G. Frye-Mason, S. Ja, A.K. Thompson, X. Fan, *Analyst (Lond)* **134**, 1386 (2009)
3. X. Sun, Y. Wang, Y. Lei, *Chem. Soc. Rev.* **44**, 8019 (2015)
4. H. Ma, F. Li, Z. Zhang, M. Zhang, *Sens. Actuators B* **244**, 1080 (2017)
5. N. Hannink, S.J. Rosser, C.E. French, A. Basran, J.A. Murray, S. Nicklin, N.C. Bruce, *Nat. Biotechnol.* **19**, 1168 (2001)
6. R.D. Luggar, M.J. Farquharson, J.A. Horrocks, R.J. Lacey, *X-Ray Spectrom.* **27**, 87 (1998)
7. D.S. Moore, *Rev. Sci. Instrum.* **75**, 2499 (2004)
8. K. Håkansson, R.V. Coorey, R.A. Zubarev, V.L. Talrose, P. Håkansson, *J. Mass Spectrom.* **35**, 337 (2000)
9. A.S. Chajistamatiou, E.B. Bakeas, *Talanta* **151**, 192 (2016)
10. A.K.M. Jamil, A. Sivanesan, E.L. Izake, G.A. Ayoko, P.M. Fredericks, *Sens. Actuators B* **221**, 273 (2015)
11. J.M. Sylvia, J.A. Janni, J.D. Klein, K.M. Spencer, *Anal. Chem.* **72**, 5834 (2000)
12. E.S. Forzani, D. Lu, M.J. Leright, A.D. Aguilar, F. Tsow, R.A. Iglesias, Q. Zhang, J. Lu, J. Li, N. Tao, *J. Am. Chem. Soc.* **131**, 1390 (2009)
13. J. Mbah, K. Moorer, L. Pacheco-Londoño, S. Hernandez-Rivera, G. Cruz, *Electrochim. Acta* **88**, 832 (2013)

14. Y.-N. Gong, L. Jiang, T.-B. Lu, *Chem. Commun. (Camb)* **49**, 11113 (2013)
15. Q. Wang, Z. Li, D.-D. Tao, Q. Zhang, P. Zhang, D.-P. Guo, Y.-B. Jiang, *Chem. Commun. (Camb)* **52**, 12929 (2016)
16. F. Akhgari, H. Fattahi, Y.M. Oskoei, *Sens. Actuators B* **221**, 867 (2015)
17. S. Rochat, T.M. Swager, *ACS Appl. Mater. Interfaces* **5**, 4488 (2013)
18. A. Rose, Z. Zhu, C.F. Madigan, T.M. Swager, V. Bulović, *Nature* **434**, 876 (2005)
19. J.-S. Yang, T.M. Swager, *J. Am. Chem. Soc.* **120**, 11864 (1998)
20. L. Feng, H. Li, Y. Qu, C. Lü, *Chem. Commun. (Camb)* **48**, 4633 (2012)
21. H. Li, Y. Zhu, J. Zhang, Z. Chi, L. Chen, C.-Y. Su, *RSC Adv.* **3**, 16340 (2013)
22. H. Siu, J. Duhamel, *Macromolecules* **37**, 9287 (2004)
23. F.M. Winnik, *Chem. Rev.* **93**, 587 (1993)
24. B. Adhikari, J. Nanda, A. Banerjee, *Chemistry (Easton)* **17**, 11488 (2011)
25. N. Maneelun, T. Vilaivan, *Tetrahedron* **69**, 10805 (2013)
26. K. Takemoto, M. Karasawa, M. Kimura, *ACS Appl. Mater. Interfaces* **4**, 6289 (2012)
27. K.P. Gan, M. Yoshio, T. Kato, *J. Mater. Chem. C* **4**, 5073 (2016)
28. E. Rodríguez-Alba, J. Ortiz-Palacios, E.G. Morales-Espinoza, M. Vonlanthen, B.X. Valderrama, E. Rivera, *Synth. Met.* **206**, 92 (2015)
29. M. Vonlanthen, A. Cevallos-Vallejo, E. Aguilar-Ortiz, A. Ruiu, P. Porcu, E. Rivera, *Polymer (UK)* **99**, 13 (2016)
30. D.P. Bhopate, P.G. Mahajan, K.M. Garadkar, G.B. Kolekar, S.R. Patil, *RSC Adv.* **4**, 63866 (2014)
31. G. Zaragoza-gala, M.A. Fowler, J. Duhamel, R. Rein, N. Solladie, E. Rivera, *Languimir* **28**, 11195 (2012)
32. G. Zaragoza-Galán, M.A. Fowler, J. Duhamel, R. Rein, N. Solladié, E. Rivera, *Langmuir* **28**, 11195 (2012)
33. T.C. Wang, N.A. Vermeulen, I.S. Kim, A.B.F. Martinson, J.F. Stoddart, J.T. Hupp, O.K. Farha, *Nat. Protoc.* **11**, 149 (2016)
34. S. Shanmugaraju, P.S. Mukherjee, *Chem. Commun. (Camb)* **51**, 16014 (2015)
35. M. Graetzel, J.K. Thomas, *J. Am. Chem. Soc.* **95**, 6885 (1973)
36. E. Miller, D. Jóźwik-Styczyńska, *Colloid Polym. Sci.* **285**, 1561 (2007)
37. J.M.G. Martinho, A.T. Reis e Sousa, M.E. Oliveira Torres, A. Fedorov, *Chem. Phys.* **264**, 111 (2001)
38. P. Beyazkilic, A. Yildirim, M. Bayindir, *Nanoscale* **6**, 15203 (2014)
39. M. Okamoto, F. Tanaka, *J. Phys. Chem. A* **106**, 3982 (2002)
40. M.W. Geiger, N.J. Turro, *Photochem. Photobiol.* **22**, 273 (1975)
41. X.-L. Ni, Y. Wu, C. Redshaw, T. Yamato, *Dalton Trans* **43**, 12633 (2014)
42. J.M.G. Martinho, *J. Phys. Chem.* **93**, 6687 (1989)
43. R.A. Beecroft, R.S. Davidson, D. Goodwin, J.E. Pratt, X.J. Luo, *J. Chem. Soc. Faraday Trans. 2* **82**, 2393 (1986)
44. C.M. Cardona, T. Wilkes, W. Ong, A.E. Kaifer, T.D. McCarley, S. Pandey, G.A. Baker, M.N. Kane, S.N. Baker, F.V. Bright, *J. Phys. Chem. B* **106**, 8649 (2002)
45. G.R. Newkome, Z. Yao, G.R. Baker, V.K. Gupta, *J. Org. Chem.* **50**, 2003 (1985)
46. G.R. Newkome, A. Nayak, R.K. Behera, C.N. Moorefield, G.R. Baker, G. Newkome, A. Nayak, R. Behera, C. Moorefield, G. Baker, *J. Org. Chem.* **57**, 358 (1992)
47. G.R. Newkome, K.K. Kotta, C.N. Moorefield, *J. Org. Chem.* **70**, 4893 (2005)
48. G.R. Newkome, C.D. Weis, C.N. Moorefield, I. Weis, *Macromolecules* **30**, 2300 (1997)
49. C.D. Schmidt, N. Lang, N. Jux, A. Hirsch, *Chemistry (Easton)* **17**, 5289 (2011)
50. U. Hartnagel, D. Balbinot, N. Jux, A. Hirsch, *Org. Biomol. Chem.* **4**, 1785 (2006)
51. C. Ornelas, R. Lodescar, A. Durandin, J.W. Canary, R. Pennell, L.F. Liebes, M. Weck, *Chemistry (Easton)* **17**, 3619 (2011)
52. F. Spänig, M. Ruppert, J. Dannhäuser, A. Hirsch, D.M. Guldi, *J. Am. Chem. Soc.* **131**, 9378 (2009)
53. D.J. Berry, Y. Ma, J.R. Ballinger, R. Tavaré, A. Koers, K. Sunassee, T. Zhou, S. Nawaz, G.E.D. Mullen, R.C. Hider, P.J. Blower, *Chem. Commun. (Camb)* **47**, 7068 (2011)
54. E. Rivero-Buceta, E.G. Doyagüez, I. Colomer, E. Quesada, L. Mathys, S. Noppen, S. Liekens, M.-J. Camarasa, M.-J. Pérez-Pérez, J. Balzarini, A. San-Félix, *Eur. J. Med. Chem.* **106**, 34 (2015)
55. H. Destecroix, C.M. Renney, T.J. Mooibroek, T.S. Carter, P.F.N. Stewart, M.P. Crump, A.P. Davis, *Angew. Chem. Int. Ed. Engl.* **54**, 2057 (2015)
56. T. Zhou, H. Neubert, D.Y. Liu, Z.D. Liu, Y.M. Ma, X.L. Kong, W. Luo, S. Mark, R.C. Hider, *J. Med. Chem.* **49**, 4171 (2006)
57. N. Dib, L. Fernández, L. Otero, M. Santo, M. Calderón, M. Martinelli, M. Strumia, *J. Inclusion Phenom. Macrocycl. Chem.* **82**, 351 (2015)
58. L. Fernandez, M. Calderón, M. Martinelli, M. Strumia, H. Cerecetto, M. González, J.J. Silber, M. Santo, *J. Phys. Org. Chem.* **21**, 1079 (2008)
59. C. Ornelas, R. Pennell, L.F. Liebes, M. Weck, *Org. Lett.* **13**, 976 (2011)
60. M.C. Strumia, A. Halabi, P.A. Pucci, G.R. Newkome, C.N. Moorefield, J.D. Epperson, *J. Polym. Sci. Part A* **38**, 2779 (2000)
61. G.R. Newkome, K.S. Yoo, C.N. Moorefield, *Des. Monomers Polym.* **5**, 67 (2002)
62. A. Amin, R. Sarkar, C.N. Moorefield, G.R. Newkome, *Polym. Eng. Sci.* **53**, 2166–2174 (2013)
63. S. Zhao, A. Ramette, G.-L. Niu, H. Liu, N.-Y. Zhou, *FEMS Microbiol. Ecol.* **70**, 159 (2009)
64. P. Paramasivan, C. Lai, C. Pickard, M. Ardern-Jones, E. Healy, P.S. Friedmann, *Br. J. Dermatol.* **162**, 594 (2010)